

## RELEVANCE OF A MULTI-SCALE APPROACH TO MONITOR ASR IN CONCRETE

Younes Boukari <sup>1,2,3</sup>, David Bulteel <sup>1,2</sup>, Patrice Rivard <sup>3</sup>, Nor-Edine Abriak <sup>1,2</sup>

<sup>1</sup> Univ Lille Nord de France, F-59000 Lille, France

<sup>2</sup> EMDouai, MPE-GCE, F-59500 Douai, France

<sup>3</sup> Université de Sherbrooke, Sherbrooke, Canada

### Abstract

This paper proposes a non conventional approach based on the combined use of non linear acoustics and physico-chemical analysis to monitor progressive ASR damage in concrete. The study was carried out on laboratory concrete specimens kept in accelerated conditions for ASR (100% R.H. and 38°C).

Non linear acoustics allowed detecting and tracking the early evolution of micro-cracking in concrete with a higher sensitivity than Young modulus (static and dynamic), while ultrasonic pulse velocity and compressive strength have still not being significantly affected.

The physico-chemical approach showed that, in the case of reactive limestone, granular swelling caused by the formation of Q<sub>3</sub> tetrahedron is responsible for early micro-cracking in concrete, when reaction products are still barely visible. In a second phase of swelling, the swelling of silica gels is then supposed to be the major cause of further cracking.

This multi-scale approach provides important information for a more accurate monitoring of ASR in concrete.

**Keywords:** Alkali-silica reaction, silica alteration, non linear acoustics, Spratt limestone

### 1 INTRODUCTION

Accurate observation and adequate interpretation of multi-scale degradations caused by alkali-silica reaction (ASR) to concrete remain a complex issue, limited by the lack of sensitive and specific monitoring techniques.

While most of the quantitative and specific methods currently used for ASR monitoring are based on petrography [1,2], a chemical method has been developed at the École des Mines de Douai (France) over the last decade [3,4]. This approach, focusing on aggregates deterioration by ASR, shows linear correlations over the reaction between the swelling of aggregates and the swelling of concrete. The physical variations observed at mesoscopic scale (swelling of aggregate) were also associated at the microscopic scale with the amorphisation of silica [5]. This phenomenon can be considered as a direct consequence of alkali-silica reaction.

---

\* Correspondence to: david.bulsteel@mines-douai.fr

At the macroscopic scale, several researchers have pointed out the potential of nonlinear acoustics/ultrasonics to assess damage in concrete [6-9]. Indeed, it was shown that porous materials, such as concrete, exhibit a nonlinear behavior, which is enhanced with the presence of cracks. Chen *et al.* suggested that nonlinear ultrasonics could quantitatively detect microcracking caused by ASR in mortar samples [10]. However, the sensitivity of these methods can also turn out to be a drawback in the case of concrete since the results can be significantly affected by various parameters (e.g. water content of concrete, cracks caused by drilling, etc.).

This paper proposes to monitor progressive ASR damage on laboratory concrete specimens. Recent techniques (physico-chemical analysis of aggregate and non linear acoustics) are compared with more classical methods, traditionally used to assess damage in concrete. The aim of this study is to demonstrate how the non conventional methods presented here allow collecting new and complementary information for a more accurate monitoring of concrete deterioration.

## 2 MATERIALS AND METHODS

### 2.1 Materials and mixture proportions

#### *Concrete mix design*

A reactive concrete mixture was made with Spratt Limestone as coarse aggregate with equal mass quantities of size fractions 20-14, 14-10 and 10-5 mm. This aggregate, well known for its reactivity, is a crushed fine-gained siliceous limestone with chalcedony inclusions and significant amount of clay. A crushed non reactive aggregate from Marbleton quarry (QC, Canada), selected for its low silica content (<2%), was used as fine aggregate.

Concrete mix was prepared with W/C ratio of 0.5, and a coarse aggregate: fine aggregate: cement = 1.89: 1.38 :1 by mass (cement content : 450 kg/m<sup>3</sup>). Reagent grade NaOH pellets were added to mixing water to increase the total alkali content to 5.62 kg/m<sup>3</sup> Na<sub>2</sub>O<sub>eq</sub>.

#### *Casting and conditioning of test specimens*

Thirty two reactive concrete samples were cast. Three prisms (75x75x300mm) were cast with stainless reference studs fixed at both ends for length measurements. Three cylinders (100x200mm) were used for non destructive testing (linear and nonlinear acoustics). Twenty four cylinders (100x200mm) were used to assess mechanical properties and physico-chemical properties of aggregates. Two cylinders (100x200mm) were used for petrographic examinations.

After 28 days in a curing room at 21°C, samples were placed over water in hermetic plastic pails to provide the humidity condition required for ASR development. The pails were stored at 38°C to accelerate the reaction. All initial measurements were taken after the curing period.

### 2.2 Methods for assessment and analysis

#### *Length change and mass variation*

Length change and mass variation of prisms have been measured periodically during fourteen month following the provisions of CSA A23.2-14A.

#### *Petrographic examination*

Petrographic examination was performed on polished concrete specimens with a stereomicroscope at a magnification of 16x. Observations were conducted according to the Damage Rating Index (DRI) method [1, 2]. This method consists in counting defects associated with ASR (e.g. cracks in aggregates, air voids lined

with gel, etc.) and associating each type of defect with a weighting factor. The DRI number is the sum of the weighed factors normalized for a 100cm<sup>2</sup> surface area.

#### *Mechanical properties*

Mechanical tests were conducted on cylinders (100x200mm) in compliance with ASTM standards to determine the compressive strength  $f_c$  (ASTM C39M), the Young modulus  $E$  (ASTM C469-02) and the splitting tensile strength  $f_t$  (ASTM C496M-04) of concrete. Two specimens were used for each mechanical test.

#### *Linear acoustics*

Linear acoustics measurements were also performed on cylinders using ASTM standard for ultrasonic pulse velocity UPV (ASTM C597) and dynamic Young modulus  $E_{dyn}$  (ASTM C215-02).

#### *Non linear resonance*

Nonlinear resonance tests were performed with the experimental device illustrated in Figure 1.

The concrete sample is excited by a sinusoidal oscillation. The signal frequency is repeatedly swept through the fundamental mode resonance peak with a progressively increasing drive amplitude. When the drive amplitude increases, the resonance peak of the concrete sample shifts toward lower values. As a highly nonlinear material, concrete naturally exhibits a frequency shift when submitted to nonlinear resonance [11]. The frequency shift increases with damage.

The nonlinear parameter  $\alpha$  (unitless) was derived from the resonance frequency shift as a function of strain:

$$\Delta f/f = (f-f_0)/f \approx \alpha \Delta \epsilon \quad (1)$$

where  $f$  is the resonance frequency,  $f_0$  the resonance frequency at the lowest (linear) drive level and  $\Delta \epsilon$  is the strain amplitude.

#### *Physico-chemical analysis*

Since the analysis of aggregates degradation is focused on the siliceous part of the aggregate, a chemical attack on crushed concrete is required to remove undesired elements [4]. The first step is a selective acid attack using a cold 1 M HCl to remove the cement paste, the calcite, the dolomite and the C-S-H/C-K-S-H phases formed by the ASR. The second step is a complexant and basic attack to remove impurities such as Fe<sub>2</sub>O<sub>3</sub> and MgO. The final step is an acid attack identical to step 1, which allows protonating the Q<sub>3</sub> sites negatively charged in the basic medium and removing residual calcite. The porous volume ( $V_p$ ) and the absolute volume ( $V_{abs}$ ) are measured on the remaining aggregate residues. The porous volume is obtained by the BJH method (Barrett, Joyner, Halenda) [12] from the nitrogen adsorption and desorption curves measured on an ASAP (Accelerated Surface Area and Porosimetry) analyzer. The absolute volume is obtained from a helium pycnometer analyzer. The apparent volume ( $V_{app}$ ) is defined as the sum of porous and absolute volumes.

Chemical alteration is also measured by thermogravimetric analysis (TGA) on the residue of the chemical attack. During the thermal treatment between 200°C and 1000°C, silanol groups (Q<sub>3</sub>) are modified to form silica (Q<sub>4</sub>) and released water:



The changes of mass loss observed between different levels of concrete expansion refer to changes of the quantity of silanols in reactive silica.

### 3 RESULTS

All the indicators presented in the previous section were measured and compared at four levels of expansion: 0% (after a 28 days curing period), 0.03%, 0.06% and 0.09%. The 0.09% expansion rate measured after fourteen months of 38°C storing at >95% R.H. was surprisingly low regarding the known high reactivity of Spratt Limestone. However, the reason why concrete specimens did not reach higher expansion could not be clearly identified.

#### 3.1 “Classical” indicators of ASR damage

The average values obtained for “classical” indicators of ASR damage are given in Table 1 (average value  $\pm$  standard deviation). Standard deviations were not calculated for mechanical properties since only two specimens were tested for each average value presented.

Petrographic examinations revealed a slight increase in the quantity of cracks, predominantly inside the aggregates particles, between initial observations and a 0.03% expansion rate. Despite a DRI increase from 8 to 23, this last value remains too low to detect formally the presence of ASR in concrete [2]. When expansion reached 0.06%, the appearance of large cracks propagating from the aggregates particles towards the cement paste (Figure 2a) and of small inclusions of silica gel allows a clear detection of ASR damage in the concrete. For a 0.09% expansion level, the presence of crack networks in a majority of the aggregates particles (Figure 2b) underlies that mechanical properties should be significantly affected by ASR.

From a macroscopic point of view, compressive strength shows a regular increase from 38.5 MPa to 46.3 MPa between initial measurement and a 0.06% expansion level, indicating that  $f_c$  is not significantly affected during this first step of cracks occurrence and propagation. At an expansion level of 0.09%,  $f_c$  finally dropped under its initial value to 37.7MPa. Tensile strength shows a slightly better - but still limited - sensitivity to ASR damage since a 14% increase is observed while the increase of  $f_t$  was of 20% (between 0% and 0.06% expansion rate). The final measurement also resulted in a decrease under initial properties. Young modulus was clearly the most sensitive mechanical properties to ASR damage since it shows a continuous decrease from 0.03% expansion, resulting in a 41% loss between initial and final measurements.

Concerning linear acoustics, UPV remains stable with a maximum variation of 3% and all average values upon 4460 m/s, inferring a constantly good quality concrete. The dynamic Young modulus shows, like static modulus, a regular reduction with the concrete expansion.

#### 3.2 Physico-chemical indicators of microscopic damage

The results of physico-chemical analysis are shown in Figures 3 (apparent volume) and 4 (mass loss during TGA). For each expansion level, six specimens were analysed.

Two main phases of swelling were observed. At the beginning of the reaction (between 0% and 0.03% expansion), the increase of average mass loss from 4.36% to 5.02% is attributed to the formation of  $Q_3$  tetrahedrons. The formation of  $Q_3$  tetrahedrons in the structure of silica, corresponding to  $Q_4 \rightarrow Q_3$  transition caused by alkaline hydroxides attack, is believed to be responsible for granular swelling [4]. No significant change in apparent volume could be observed during this period.

When the expansion reached 0.06%, the mass loss stabilized while the apparent volume underwent a 5% increase. These changes can be associated with a transition in the degradation process, during which the dissolution of silica ( $Q_3 \rightarrow Q_0$ ) becomes prevailing over its amorphization. This trend seems to be confirmed by the last mass loss measurements (0.09% expansion), which show a clear decrease down to 3.61%. This

indicates that the dissolution should then be the prevailing chemical reaction with regards to reactive silica alteration. For this level of expansion, apparent volume couldn't be estimated properly since the changes in the size of porosity made porous volume measurement unsuited to the ASAP analyzer range.

### 3.3 Non linear indicator of mesoscopic/macroscopic damage

An example of the diagrams used to generate  $\alpha$  value is shown in Figure 5 (sample n°3 at 0% and 0.09% expansion rate). Results of nonlinear measurements are given in Figure 6. Non linear parameter  $\alpha$  shows a much higher sensitivity to microcracking than the other "classical" macroscopic indicators monitored (mechanical properties, linear acoustics). A 176% increase was observed at an expansion level of only 0.03% while the variation of the second most sensitive parameters tested (the static Young modulus) was 15%.

For further expansion levels, the variation of average values of  $\alpha$  remains about ten times higher than the variations of any other damage indicator. Nevertheless, the more concrete is damaged, the harder the different levels of deterioration can be distinguished. This observation is mainly attributed to the increasing heterogeneity between different samples when damaged. The presence of alkali-silica gel in the cracks of the concrete with increasing expansion has no significant influence on  $\alpha$  values and, in general, on fast dynamics indicators. Let us mention that a recent study showed that the presence alkali-silica gel in concrete could be monitored with slow dynamics experiments [13].

## 4 DISCUSSION

The results obtained with the "classical" indicators were fairly expected since the better sensibility of elastic properties compared with compressive strength or ultrasonic pulse velocity has already been demonstrated and discussed in previous papers [14-16]. In this case study, these indicators were mainly used as a reference to point out the additional information provided by physico-chemical analysis and non linear acoustics.

Petrographic examination remains a reliable method to identify ASR when used as a qualitative tool. Using the DRI method as a quantitative tool has already showed good correlations with expansion measurements [2], but its dependence on the petrographer qualifications still represents a major issue to make petrographic examination a reliable quantitative method. Physico-chemical analysis is, with *the Stiffness Damage Test* mechanical approach [17,18], some rare existing alternative to microscopy that can provide quantitative information specific to ASR. The different phases of swelling identified in this study differ from previous work, in which reactive aggregates were undergoing an apparent volume and mass loss increase until asymptotic swelling [4,19]. This difference can be attributed to the specificity of each aggregate and to the difference in the accelerated tests used. The quantitative information collected allowed a more accurate interpretation of microscopic/mesoscopic degradation process, although it cannot be extended to other types of aggregates or concrete mix design. Further investigation on a larger variety of reactive aggregates is now necessary to identify whether other types of physico-chemical deterioration can be identified. The objective would be to define "families" of reactive aggregates depending on their ASR degradation process.

The use of non linear acoustics has complemented this investigation by providing an extremely clear view on concrete progressive macroscopic deterioration, especially for early damage. Very little work has been carried out to link non linear indicators to ASR [10], the present study confirmed the great potential of these non-destructive techniques to track progressive cracking due ASR with higher accuracy. Although a resonance test is not really suitable for *in situ* observations, this technique should be particularly suitable for rapid reactivity evaluations or residual expansion tests. Residual expansion tests on concrete cores drilled from in service structure are being carried on, as well as reproducibility tests (based on varying water content in concrete).

## 5 CONCLUSIONS

The present paper aimed at demonstrating the relevance of recent monitoring methods to provide complementary information on the progressive deterioration of concrete affected by ASR. It was shown that:

- Physico-chemical analysis of aggregate allowed complementing the specific information from petrographic examination by providing quantitative values on silica deterioration rate. This tracking provides important clue for a more complete interpretation of chemical degradation process in concrete due to ASR.
- Non linear resonance was about ten times more sensitive to concrete cracking than any other macroscopic indicator used.

The use of physico-chemical analysis and non linear resonance, combined with “classical” indicators of ASR damage, allowed an accurate tracking and interpretation of degradation process caused by ASR considering current knowledge.

## 6 REFERENCES

- [1] Grattan-Bellew, P.E (1995): Laboratory evaluation of alkali-silica reaction in concrete from Saunders Generating Station. *ACI Materials Journal* (92): 126-134.
- [2] Rivard, P, and Ballivy, G (2005): Assessment of the expansion related to alkali-silica reaction by the Damage Rating Index method. *Construction and Building Materials* (19): 83-90.
- [3] Bulteel, D, Garcia-Diaz, E, Vernet, C, and Zanni, H (2002): Alkali-silica reaction: a method to quantify the reaction degree. *Cement and Concrete Research* (32): 1199-1206.
- [4] Garcia-Diaz, E, Riche, J, Bulteel, D, and Vernet, C (2006): Mechanism of damage for the alkali-silica reaction. *Cement and Concrete Research* (36): 395-400.
- [5] Verstraete, J, Khouchaf, L, Bulteel, D, Garcia-Diaz, E, Flank, A.M., and Tuilier, M.H (2004): Amorphisation mechanism of a flint aggregate during the alkali-silica reaction: X-ray diffraction and X-ray absorption XANES contributions. *Cement and Concrete Research* (34): 581-586.
- [6] Van Den Abeele, K, and De Visscher, J (2000): Damage assessment in reinforced concrete using spectral and temporal nonlinear vibration techniques. *Cement and Concrete Research* (30): 1453-1464.
- [7] Payan, C, Garnier, V, Moysan, J, and Johnson, P.A (2007): Applying nonlinear resonant ultrasound spectroscopy to improving thermal damage assessment in concrete. *Journal of the Acoustical Society of America* (121): EL125-EL130.
- [8] Stauffer, J.D, Woodward, C.B, and White, K.R (2005): Nonlinear ultrasonic testing with resonant and pulse velocity parameters for early damage in concrete. *ACI Materials Journal* (102): 118-121.
- [9] Bentahar, M, El Aqra, H, El Guerjouma, R, Griffa, M, and Scalerandi, M (2006): Hysteretic elasticity in damaged concrete: Quantitative analysis of slow and fast dynamics. *Physical Review B* (73): 014116.
- [10] Chen, X.J, Kim, J.Y, Kurtis, K.E, Qu, J, Shen, C.W, and Jacobs, L.J (2008): Characterization of progressive microcracking in Portland cement mortar using nonlinear ultrasonics. *NDT & E International* (41), 112-118.
- [11] Guyer, R.A, and Johnson, P.A (1999): Nonlinear mesoscopic elasticity: Evidence for a new class of materials. *Physics Today* (52), 30-36.
- [12] Barrett, E.P, Joyner, L.G, and Halenda, P.P (1951): The determination of pore volume and area distributions in porous substances. i-computations from nitrogen isotherms. *Journal of the American Chemical Society* (73): 373-380.
- [13] Kodjo, A.S, Rivard, P, Cohen-Tenoudji, F, Gallias, J-L (2011): Impact of the alkali-silica reaction products on slow dynamic behavior of concrete. *Cement and Concrete Research* (41): 422-428.
- [14] Swamy, R.N, and Alasali, M.M (1988): Engineering properties of concrete affected by alkali-silica reaction. *ACI Materials Journal* (85): 367-374.
- [15] Ahmed, T, Burley, E, Rigden, S, and Abu-Tair, A.I (2003): The effect of alkali reactivity on the mechanical properties of concrete. *Construction and Building Materials* (17): 123-144.

- [16] Sargolzahi, M, Kodjo, S.A, Rivard, P, and Rhazi, J (2010): Effectiveness of nondestructive testing for the evaluation of alkali-silica reaction in concrete. *Construction and Building Materials* (24): 1398-1403.
- [17] Chrisp, T. M, Waldron, P, Wood, J. G. M (1993): Development of a Nondestructive Test to Quantify Damage in Deteriorated Concrete. *Magazine of Concrete Research* (45): 247-256.
- [18] Smaoui, N, Berube, M. A, Fournier, B, Bissonnette, B, Durand, B (2004): Evaluation of the expansion attained to date by concrete affected by alkali-silica reaction. Part I: Experimental study. *Canadian Journal of Civil Engineering* (31): 826-845
- [19] Monnin, Y, Degrugilliers, P, Bulteel, D, and Garcia-Diaz, E (2006): Petrography study of two siliceous limestones submitted to alkali-silica reaction. *Cement and Concrete Research* (36): 1460-1466.

**7 ACKNOWLEDGEMENT**

Authors wish to thank Apedovi Kodjo and Idriss Moundougou for their respective contributions on nonlinear acoustics and physico-chemical tests. Financial support has been provided by the Natural Science & Engineering Research Council of Canada (NSERC).

Table 1 : Evolution of "classical" ASR damage indicators with concrete expansion

Expansion	f 'c (MPa)	f 't (MPa)	E (GPa)	UPV (m/s)	E <sub>dyn</sub> (GPa)	DRI
<b>0%</b>	38.5	3.4	30.5	4570 ± 14	35.5 ± 0.3	8
<b>0.03%</b>	42.2	3.8	26.0	4487 ± 50	32.5 ± 0.4	23
<b>0.06%</b>	46.3	3.9	25.0	4477 ± 65	31.8 ± 0.1	67
<b>0.09%</b>	37.7	3.2	18.0	4602 ± 45	30.6 ± 0.2	118

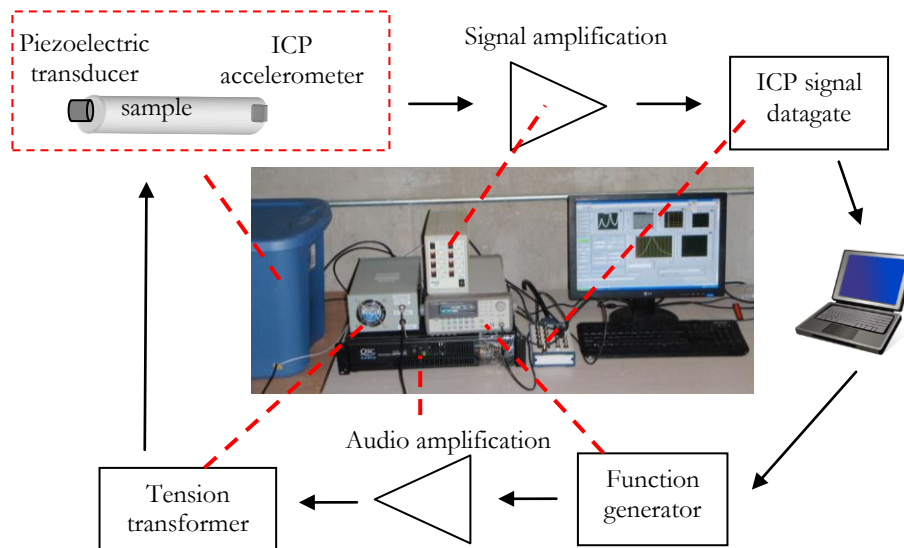


FIGURE 1: Experimental device for non linear resonance tests

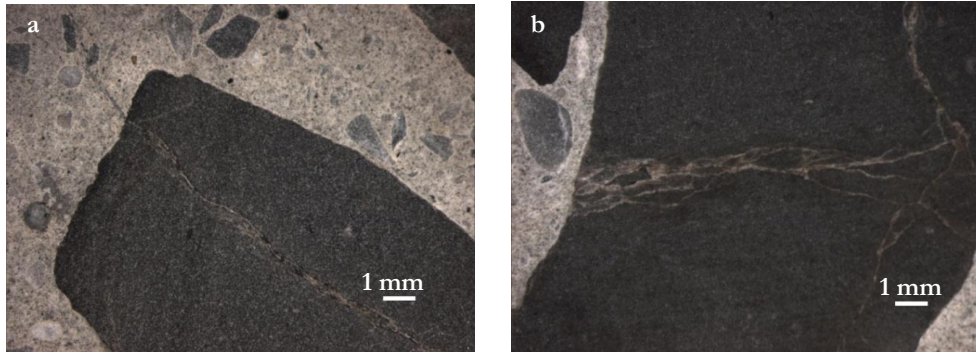


FIGURE 2: Typical petrographic features observed for 0.06% expansion (a) and 0.09% expansion (b)

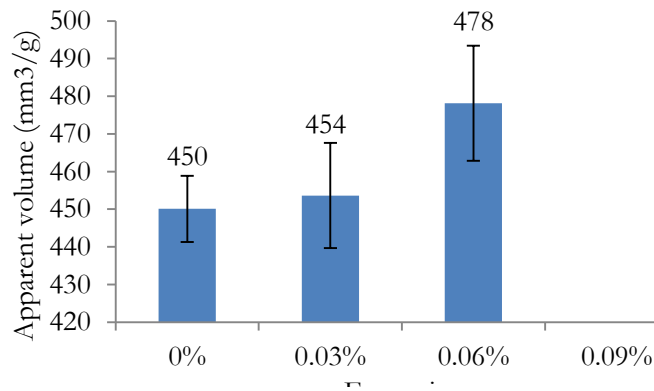


FIGURE 3: Evolution of the apparent volume of reactive silica with expansion

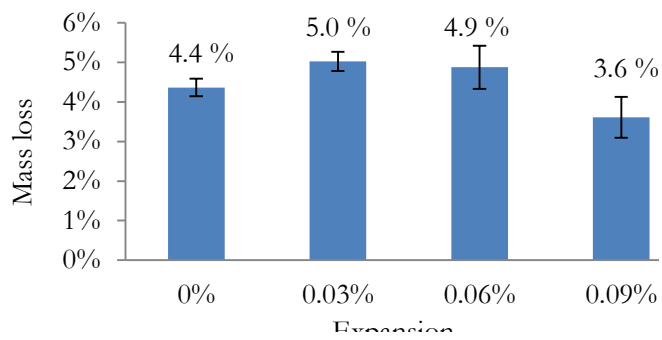


FIGURE 4: Evolution of the mass loss of reactive silica during TGA with expansion

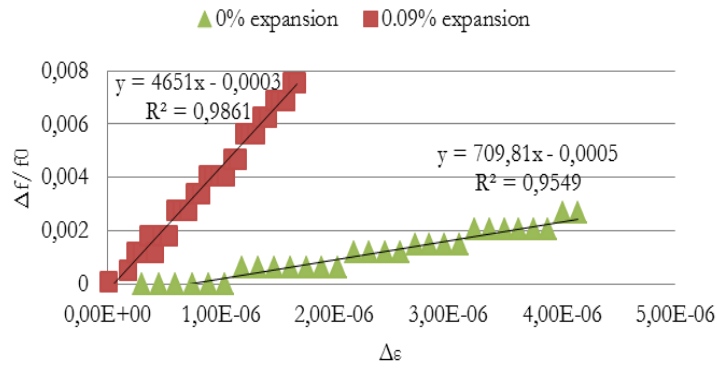


FIGURE 5: Determination of  $\alpha$  value for sample n°3 at 0% and 0.09% expansion

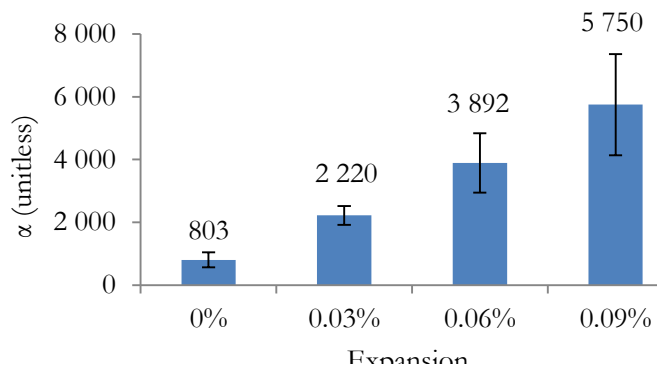


FIGURE 6: Evolution of nonlinear parameter  $\alpha$  with expansion